Cerebral Cortex January 2012;22:1–12
doi:10.1093/cercor/bhr018
Advance Access publication May 25, 2011

Total and Regional Brain Volumes in a Population-Based Normative Sample from 4 to 18 Years: The NIH MRI Study of Normal Brain Development

Brain Development Cooperative Group

Address correspondence to Nicholas Lange, Neurostatistics Laboratory, McLean Hospital, 115 Mill Street, Belmont, MA 02478, USA. Email: nlange@hms.harvard.edu.

Using a population-based sampling strategy, the National Institutes of Health (NIH) Magnetic Resonance Imaging Study of Normal Brain Development compiled a longitudinal normative reference database of neuroimaging and correlated clinical/behavioral data from a demographically representative sample of healthy children and adolescents aged newborn through early adulthood. The present paper reports brain volume data for 325 children, ages 4.5–18 years, from the first cross-sectional time point. Measures included volumes of whole-brain gray matter (GM) and white matter (WM), left and right lateral ventricles, frontal, temporal, parietal and occipital lobe GM and WM, subcortical GM (thalamus, caudate, putamen, and globus pallidus), cerebellum, and brainstem. Associations with cross-sectional age, sex, family income, parental education, and body mass index (BMI) were evaluated. Key observations are: 1) age-related decreases in lobar GM most prominent in parietal and occipital cortex; 2) age-related increases in lobar WM, greatest in occipital, followed by the temporal lobe; 3) age-related trajectories predominantly curvilinear in females, but linear in males; and 4) small systematic associations of brain tissue volumes with BMI but not with IQ, family income, or parental education. These findings constitute a normative reference on regional brain volumes in children and adolescents.

Keywords: adolescents, brain volumes, children, healthy, MRI

Introduction

The National Institutes of Health (NIH) Magnetic Resonance Imaging (MRI) Study of Normal Brain Development was initiated to provide a resource for the scientific community with which to address questions related to healthy pediatric brain development and further develop image-processing tools. This longitudinal multisite project, conducted by the Brain Development Cooperative Group (BDCG), is establishing a comprehensive, multimodal database of pediatric structural MRI, diffusion tensor imaging, and proton MR spectroscopy data together with concurrent clinical/behavioral data. The study employed a population-based strategy to recruit a sample that mirrored the demographic distribution of the US population. Imaging assessments were obtained in conjunction with comprehensive documentation of demographic characteristics and assessments of clinical/behavioral characteristics (BDCG 2006; Waber et al. 2007).

The project comprises 2 coordinated protocols: "Objective 1," the subject of this report, enrolled children and adolescents from 4 years and 6 months to 18 years and 3 months of age; "Objective 2," performed at a subset of the Objective 1 study sites, enrolled newborns, toddlers, and preschoolers up to the age of 4 years, 5 months, thereby providing continuity with Objective 1 (Almli et al. 2007). Both protocols included an accelerated longitudinal design (Harezlak et al. 2005) with multiple imaging and clinical/behavioral assessments and scanning and clinical/behavioral protocols repeated at intervals ranging from months to years, depending on the age of the child. Although similar domains of cognitive/behavioral functioning were evaluated in the Objective 1 (older) and Objective 2 (younger) cohorts, specific age-appropriate clinical/behavioral measures differed between them. More importantly, due to brain tissue contrast differences between the 2 cohorts, the imaging protocols were necessarily different. The contrast differences, particularly for the very young ages (<3 years of age) require specialized segmentation algorithms for this population, which are under development. Given the differences in clinical/behavioral measures, MRI protocols, and image processing methods, results from Objective 2 data are not published here.

This report addresses cross-sectional age- and sex-related differences in whole- and regional brain volumes and relationships to key socioeconomic and physical growth indicators for a demographically representative sample of 325 children, ages 4 years and 9 months through 18 years and 4 months based on data from the first cross-sectional time point for Objective 1. As such, it constitutes a normative reference for studies of healthy brain development and brain-based disorders derived from a larger data set and resource that is freely available to qualified researchers (www.NIH-PediatricMRI.org); see Data Access.

Materials and Methods

Participants

Healthy children and adolescents ($N = 433$) were enrolled in Objective 1 at 6 Pediatric Study Centers (PSCs) across the United States: Children's Hospital, Boston; Children's Hospital Medical Center of Cincinnati; Children's Hospital of Philadelphia; the University of California at Los Angeles; the University of Texas Health Science Center at Houston; and Washington University Saint Louis. A Data Coordinating Center (DCC) at the Montreal Neurological Institute coordinated the imaging aspects of the study and consolidated the data into a centralized database. A Clinical Coordinating Center at Washington University Saint Louis coordinated the recruitment for the project and managed the clinical/behavioral arm of the study. Institutional Review Boards at all participating institutions approved all study protocols. Informed consent was obtained from parents or guardians and participants of adult age.

A population-based sampling plan was implemented to minimize biases that can be present in samples of convenience and thus maximized the generalizability of the findings. Data from the 2000 US Census (United States Census Bureau 2000) were used in conjunction with site-specific zip code–based demographic data (geocoding) to develop regional targets for recruitment (BDCG 2006). In order to achieve a sample that approximated the demographics of the US population, zip codes within a 30- to 60-mile distance of each PSC were used to compile a demographic profile for each region by income,

ethnicity, and race. These profiles were used in conjunction with national demographic data to develop a target sampling plan that defined the number of families to be recruited from low-, medium-, and high-income families. Ranges for low-, medium-, and high-income zip codes were chosen based on the Census. The sampling plan combined cross-sectional and accelerated longitudinal study design principles (Harezlak et al. 2005; BDCG 2006) and yielded a demographically representative, population-based healthy sample referenced to the Census. Volunteers were recruited into predetermined cells, whose distribution, based on family income levels (categorized as low, medium, and high) and race/ethnicity proportions within each level, approximated that of the Census. Low-income families (~25% of the sample) generally fell below the qualifying income for federal assistance (~1.5 times the poverty level), high-income families (~35%) were approximately 3 times the poverty level or higher, and medium-income families (~41%) were those in between (United States Department of Housing and Urban Development 2003). Equal numbers of males and females were targeted for each cell. As families were screened for recruitment, adjustments were made to account for regional differences in the cost of living and for family size using methods established by the Department of Housing and Urban Development (HUD). The recruitment process is described in greater detail elsewhere (BDCG 2006; Waber et al. 2007; www.NIH-PediatricMRI.org).

Following the mailing of an introductory letter, rates of successful contact were similar across income groups. However, high-income families had elevated rates of initial and total refusals relative to medium- and low-income families across various stages of the recruitment process. In contrast, exclusion rates were higher in low-income zip codes relative to middle- or high-income zip codes during the early stages of screening involving interviews for health-related factors and the completion of the Child Behavior Checklist (CBCL) to screen for exclusionary behavioral difficulties (Waber et al. 2007).

Strict and comprehensive inclusion/exclusion criteria were specified, representing factors that are established or suspected to adversely impact healthy brain development or that could prohibit completion of the full study protocol, for example, contraindications for MR scanning. Health and behavioral exclusions involved prenatal, birth, and perinatal history (including maternal substance use during pregnancy), medical and psychiatric disorders (e.g., attention deficit hyperactivity disorder (ADHD), internalizing/externalizing disorders, diabetes), poor academic functioning (e.g., special education placement), IQ < 70 (as measured with the Wechsler Abbreviated Scale of Intelligence), and a history of specific family medical and psychiatric disorders in first-degree relatives. Children with heights, weights, or head circumferences below the third percentile were excluded, but no upper limits were imposed. Detailed descriptions of inclusion/exclusion criteria have been previously reported (BDCG 2006; Waber et al. 2007). As noted above, exclusion rates were highest for low-income children.

Income and parental education (highest level of education achieved by either parent) were evaluated as predictors of brain volumes. Following enrollment, a continuous adjusted family income (AFI) variable that took into account both regional differences in the cost of living and the child's family size was derived for use in these analyses using data available from the US Department of HUD. Families with greater than four 4 members had their income adjusted downward by a percentage per family member, whereas those with fewer than four 4 family members had their income adjusted upward under the rationale that these numbers reflect income as related to need. This continuous AFI variable was computed as follows:

$$\mathrm{AFI} = ((A/B)/C\ ) \times D$$

where Variable A is the midpoint of each family's self-reported income bracket, Variable B is the HUD adjustment factor for family size, Variable C is the local median family income for the Metropolitan Statistical Area in which the family resided at the time of the interview, and Variable D is the US median family income.

Body mass index (BMI), calculated as (Weight in kg)/(Height in m)^2, served as an indicator of adiposity and was used in the analyses. Age- and sex-specific norms for BMI from 2000 available from the Centers for Disease Control (CDC) (http://www.cdc.gov/healthyweight/assessing/bmi/childrens_bmi/about_childrens_bmi.html) were used to classify individuals as underweight (less than the fifth percentile), normal weight (5th to 84th percentile), overweight (85th to 94th percentile), or obese (>94th percentile) for descriptive purposes. Of the 173 females included in the analyses, 119 (69%) had a BMI within the normal range for sex and age, 4 (2%) were underweight, 30 (17%) were overweight, and 20 (12%) were classified as obese. Of the 152 males included in the analyses, 110 (72%) had a BMI within the normal range for sex and age, 7 (5%) were underweight, 17 (11%) were overweight, and 18 (12%) were obese.

Following the application of image quality control and an automated processing pipeline, complete multispectral MRI data sets (consisting of acceptable T1, T2, and proton density (PD) scans; see below) from 325 participants were analyzed for this report. Data set exclusions due to incomplete scanning sequences or inadequate quality were found to occur at random with respect to age ($P = 0.32$) and sex ($P = 0.50$). Table 1 summarizes sample distributions for the 325 participants by age, sex, family income, and race/ethnicity.

MRI Protocols

MR brain images at 1.5 T were acquired at the 6 PSC sites without sedation with a 30- to 45-minute protocol (Table 2 and BDCG 2006). A whole-brain 3D T1-weighted spoiled gradient recalled echo sequence was applied to obtain sagittal slices with 1 mm in-plane resolution. Slice thickness was 1 mm on Siemens scanners and 1.4–1.8 mm on GE scanners, due to the width of the subject's head and the 124 slice number limit of the GE scanners. To provide additional data for use in automated multispectral tissue classification and segmentation, a dual contrast, proton density– and T2-weighted acquisition with an optimized 2D multislice (2 mm) dual echo fast spin echo sequence was obtained in the axial plane parallel to the anterior commissure-posterior commissure line.

Where feasible, children who were unable to complete the scanning protocol successfully were scanned with a "fallback" protocol consisting of shorter 2D acquisitions (Table 2). Following a careful statistical check to assure that the inclusion or exclusion of the fallback scans did not significantly modify associations between structural volumes and the demographic characteristics that guided sample selection, these scans were included in the analyses reported here. Of the total sample, 9.9% ($n = 34$) of participants contributed T1W or T2W fallback scans, 9.3% ($n = 32$) contributed both T1W and T2W fallback scans.

MRI Analysis

Following visual inspection of the data at the scanner, the scans were transferred to the DCC, where further quality control assessments using 3D display software were implemented to insure completeness of data transfer, protocol compliance, checks for motion, signal-to-noise ratio, magnetic susceptibility and other artifacts, resulting in a sample size of 401. The multimodal data collected from each subject were submitted to a series of image preprocessing steps to minimize these artifacts. First, any multislice data that were distorted by interpacket misregistration were re-registered, realigned and resampled onto a 1-mm isotropic grid (Gedamu et al. 2008). Each modality (T1, T2, and PD) was corrected in native space for 3D intensity nonuniformity using the N3 method (Sled et al. 1998). The intensity ranges of all volumes were trimmed and normalized to range 0–100 by a linear mapping of the 99.8th percentile to 100 and the 0.02th percentile to zero.

For each subject, a mutual information–based registration procedure was used to compute the rigid body transformation mapping the multiecho T2/PD volume onto the T1 volume. All data were normalized into the Talairach-like MNI stereotaxic space (Collins et al. 1994) in order to account for differences in position, orientation, and size of each subject's brain in the native scans. Although making brain sizes more comparable, the stereotaxic transformation did not, however, equate them across subjects. The T1 volume for each subject visit was mapped linearly to the stereotaxic space defined by the ICBM152 nonlinear average template using the "mritotal" program from the "mni_autoreg" software package (packages.bic.mni.mcgill.ca) with a 9-parameter transformation (3 translations, 3 rotations, and scales; Collins et al. 1994). The "mritotal" program determined the 9

Table 1
Demographic characteristics of the study sample.

		Sex								
		Male	Female							
Panel A										
	Sample size (N = 325)	152	173							
	Age (years)[a]	11.00 (3.80)	10.87 (3.71)							
	AFI[b] ($)	69 656 (29 305)	75 261 (34 084)							
	Full-scale IQ	111.27 (12.8)	111.18 (11.7)							
	BMI[c]	19.07 (4.31)	19.41 (4.29)							
	Right handed (%)	85.43 (0.03)	90.17 (0.023)							
	Parental education[d]									
	Less than high school	1	0							
	High school	18	11							
	Some college	33	38							
	College Degree	46	54							
	Some graduate school	9	13							
	Graduate school	45	55							
	No reported	0	2							
Panel B										
	AFI[b]	<$50 000		$50 000– 100 000		>$100 000		Total		
	Sex	Male	Female	Male	Female	Male	Female	Male	Female	Total
	Age (years)									
	4.8–6	2	6	11	3	0	4	13	13	26
	6–8	6	10	16	20	8	5	30	35	65
	8–10	5	8	14	12	4	7	23	27	50
	10–12	4	10	17	14	0	11	21	35	56
	12–14	12	1	10	10	4	10	26	21	47
	14–16	9	6	9	10	4	5	22	21	43
	16–18.3	6	7	6	9	5	5	17	21	38
	Total	44	48	83	78	25	47	152	173	325
Panel C										
Race/ethnicity of child		Male (n=152)	Female e (n=173)	Total (n=325)						
	American Indian or Alaskan native	3	2	5						
	Asian	2	4	6						
	Native Hawaiian or other Pacific islander	1	1	2						
	Black or African American	11	19	30						
	White	120	120	240						
	Mixed/unknown or not reported	15	27	42						
	Hispanic (of any race)	21	22	43						

[a]Mean (SD).
[b]As originally reported by telephone interview and adjusted for family size and geographical region.
[c]BMI, defined as mass (kg)/height $(m)^2$.
[d]Highest level attained by either parent.

Table 2
MRI protocols

	3DT1 weighted	2D PD/T2 weighted	Fall-back: T1 weighted	Fall-back: 2D PD/T2 weighted
Sequence	3D RF-spoiled gradient echo	Fast/turbo spin echo (ETL/turbo factor 8)	Spin echo	Fast/turbo spin echo (ETL/turbo factor 8)
Time repetition (ms)	22–25	3500	500	3500
Time echo (TE) (ms)	10–11		12	
Excitation pulse (°)	30	90	90	90
Signal averages	1	1	1	1
TE1 (effective) (ms)		15–17		15–17
TE2 (effective) (ms)		5–119		5–119
Refocusing pulse (°)	180	180	180	180
Orientation	Sagittal	Oblique axial (AC–PC)	Oblique axial (AC–PC)	Oblique axial (AC–PC)
Thickness, gap (mm)	1, 0	2, 0	3, 0	3, 0
Number of slices	Ear to ear	Apex to below cerebellum	Apex to below cerebellum	Apex to below cerebellum
Field of view (mm)	AP:256, LR:160–180 (whole head)	AP: 256, LR: 224	AP: 256, LR: 192	AP: 256, LR: 192
Matrix (mm)	AP:256, LR: for 1 mm isotropic	AP: 256, LR: 224	AP: 256, LR: 192	AP: 256, LR: 192
Scan time (min) time varies with head size	15–18	7–11	3–5	4–7

Note: AC–PC, anterior commissure-posterior commissure.

transformation parameter values that maximized the cross-correlation intensity between the subject's T1 volume and the ICBM152 template. The native T1 volume was resampled using a trilinear resampling kernel onto a standard 1-mm^3 isotropic 181 × 217 ×181 grid defined in MNI stereotaxic space. The T2-to-T1 transformation was composed with the T1 stereotaxic transformation and mapped the T2 and PD volumes to the MNI stereotaxic space to yield a voxel-by-voxel transformed T1 volume.

Once in MNI stereotaxic space, a brain extraction tool was used to create a mask of the average of the T1, T2, and PD volumes for each subject visit to remove extracerebral tissue (Smith 2002). The combination of the 3 volumes resulted in more robust segmentations than when using the T1 volume alone. The mask covered the entire cerebrum, cerebellum, and brainstem, ending at the foramen magnum. A tissue label, either white matter (WM), gray matter (GM), or cerebrospinal fluid (CSF), was assigned to each voxel within the brain mask using the Intensity Normalized Stereotaxic Environment for the Classification of Tissue program (Zijdenbos et al. 2002; Cocosco et al. 2003), using predefined locations in stereotaxic space to identify likely samples of each tissue type. The approach to tissue classification was

thus driven primarily by the expected locations of GM and WM tissues and CSF and was more robust than methods that use a standard intensity range. Although the standard GM, WM, and CSF sampling coordinates were derived from adult subjects, they were transformed to the younger subjects' MRI scans, yielding less-biased results. After a pruning process (Cocosco et al. 2003), the samples were processed by a neural net classifier to identify GM, WM, and CSF within the intracranial cavity. Total brain volume (TBV) was defined as the sum of whole-brain GM and whole-brain WM volume, including the cerebrum, cerebellum, and brainstem (ending at the foramen magnum).

Although the preceding well-established methodology has been widely used in the analysis of structural brain data from pediatric subjects, changes in MR signal intensity associated with brain maturation may have affected the likelihood of a structure being classified as GM or WM. It is plausible that immature WM may have a signal intensity that increases the likelihood of its classification as GM such that a reported decrease in GM volume may reflect a change in the size of an immature WM compartment that has been misclassified as GM. The use of the terms "GM" and "WM" volumes in the remainder of this paper refers to the above operational definitions, while acknowledging that immaturities of WM development may have affected these tissue classifications.

Brain structure segmentation was achieved with Automatic Nonlinear Image Matching and Anatomical Labeling (Collins et al. 1995; Collins and Evans 1997). The registration-based stereotaxic strategy aligned a subject's transformed T1 volume nonlinearly to a prelabeled template using a multiscale approach. The anatomical labels were then mapped through the inverse of the recovered transformation from the template onto the subject's data in the MNI stereotaxic space. The intersection of these regions with the GM, WM, and CSF tissue classes was then used to identify individual structures. These structures included the left and right frontal, temporal, parietal and occipital lobes, lateral ventricles; thalamus (dorsal thalamus), caudate (head and body), putamen, globus pallidus, cerebellum as well as brainstem. The caudate volume did not include the tail, due to the limited reliability of small-structure segmentation of 1-mm^3 1.5-T data. Four whole-brain, regionally segmented images collected from 2 males and 2 females scanned at 5 and 14 years of age are provided as Supplementary Data. The linear scaling factors estimated in the initial linear stereotaxic transformation were used to recover the native volumes for each structure.

Each step of the image processing pipeline was evaluated qualitatively. For example, ICC masking failed if part of the bone marrow, skull, or optic nerve was included. Stereotaxic registration failed if the orientation, position or size was inappropriate. T2/PD to T1 registration failed if the CSF visible in the T2 image did not line up perfectly with the sulci on the T1 data. Nonlinear registration (and the resulting segmentation) failed if the nonlinearly resampled data did not align well with the template or if the segmented lobe borders did not fall in line with the appropriate sulci or the segmented basal ganglia did not align with the borders of the corresponding structures on the subject's MRI. Of the 401 complete (T1/T2/PD) individual data sets submitted to the multistep image processing pipeline, 76 failed to meet image quality control standards for one or more steps in the pipeline, resulting in a sample size of $N = 325$ for the present report.

Biostatistical Analysis

Initial descriptive statistics by age and sex were generated based on native, unadjusted brain volume measurements. Preliminary analyses revealed large differences in the variances of regional volumes ($P < 0.0001$, Bartlett's T), which were proportional to regional means for all structures (Pearson's $r > 0.90$). The coefficient of variation (CV), defined as the standard deviation (SD) expressed as a percentage of the mean (CV = SD/mean × 100), was therefore used as the measure of variability to permit comparisons of variability across brain structures on the same scale (Lange et al. 1997; Van Belle and Fisher 2004).

Mixed-effects models (Laird and Ware 1982; Lange and Laird 1989; Venables and Ripley 2002) were applied to evaluate the simultaneous effects of age, sex, AFI, parental education, and BMI on brain volumes. The simultaneous inclusion of variables that could potentially influence brain volumes provides greater precision in the estimates of the effects of each of these predictors. Race and ethnicity were not included in these models because many cell occupancies were too small to yield reliable estimates. TBV served as a covariate for the analysis of regional brain volumes, and hemisphere/side (left vs. right) as a within-subject repeated measure under a compound symmetric variance–covariance structure for the volumes of the 4 lobes, lateral ventricles, subcortical GM and cerebellum. Linear models without random effects were employed for TBV, whole-brain GM, whole-brain WM, and brainstem volumes. The best-fitting yet simplest model for each structure was obtained by uniform application of the Akaike Information Criterion (AIC; Akaike 1974) across all structures. A testwise false-positive error rate was set at 0.05, thus controlling for potential experimentwise errors. All data analysis was performed in R version 2.10.1 (12/14/09 build; http://www.rproject.org/foundation/main.html), whose results are equivalent to those produced by SAS.

Based on reported effect sizes (Lange et al. 1997), we estimate that our sample size ($N = 325$) had probative power of at least 80% to detect regional age- and sex-related variation in all measured structures at all ages at a false-positive error rate of 5%.

Results

Descriptive Statistics

Table 3 provides average native volumes (not adjusted for TBV) and coefficients of variation for key structures. Considerable variability in the volumes was seen across measures with the lateral ventricles showing the highest volumetric variability. Figure 1 displays individual data points and best-fitting age curves separately for males and females for all regional volumes without consideration of any other covariates. Table 4 shows volumes for each year of age for males and females, represented as a percentage of the averaged 17- to 18-year value. Because of the sparse numbers of individuals in some cells, these values are more uneven across the age range than the fitted curves shown in Figure 1. Nonetheless, general patterns can be discerned consistent with the fitted curves.

For males, the best-fitting models of age-related changes in brain volumes were predominantly linear. Linear volumetric relationships were seen for TBV, whole-brain WM, frontal lobe WM, parietal lobe GM and WM, temporal lobe GM and WM, occipital lobe GM and WM, the caudate, putamen, and lateral ventricles. The best-fitting models were curvilinear (quadratic, in the shape of an inverted-U curve) for whole-brain GM, subcortical GM, frontal lobe GM, thalamus, globus pallidus, cerebellum, and brainstem. No additional or higher-order associations were found.

For females, age-related changes were more predominantly quadratic, also in the shape of an inverted-U curve. Linear volumetric relationships were seen for occipital GM, parietal WM, putamen, globus pallidus, and the lateral ventricles. Quadratic volumetric relationships were seen for TBV, whole-brain GM and WM, frontal WM, temporal GM and WM, parietal GM, occipital WM, subcortical GM, thalamus, caudate, cerebellum, and brainstem. No additional or higher-order associations were found.

Multiple Regression Analyses

The multiple regression models provided the best estimate of age and other associations because they adjusted simultaneously for the additional measured sources of variance available. Table 5 summarizes the results of the mixed models that considered covariances by age, sex, and hemisphere simultaneously in a group analysis. To simplify viewing, only estimates (regression coefficients) that were statistically significant are listed in the table. The initial set of models also

Table 3
Means and coefficients of variation (CVs) for brain volumes

Volume (cm^3)	Total (N = 325)			Male (n = 152)			Female (n = 173)		
	T	RH	LH	T	RH	LH	T	RH	LH
A. Mean									
Total brain[a]	1262.43	—	—	1327.96	—	—	1204.86	—	—
Whole-brain GM	787.13	—	—	824.48	—	—	754.31	—	—
Whole-brain WM	475.30	—	—	503.48	—	—	450.55	—	—
Lobar GM	635.34	317.7	317.64	665.97	332.86	333.11	608.43	304.38	304.04
Frontal	265.81	133.12	132.69	278.54	139.49	139.05	254.62	127.52	127.10
Parietal	136.40	67.78	68.62	143.10	70.94	72.16	130.51	65.01	65.50
Temporal	173.22	87.60	85.62	180.98	91.51	89.48	166.40	84.17	82.23
Occipital	59.92	29.20	30.71	63.35	30.93	32.42	56.90	27.69	29.21
Lobar WM	394.18	196.87	197.31	418.49	209.16	209.34	372.82	186.07	186.75
Frontal	170.04	84.75	85.29	180.54	90.00	90.53	160.82	80.13	80.69
Parietal	93.07	46.40	46.67	98.70	49.16	49.54	88.12	43.96	44.16
Temporal	85.93	43.28	42.65	90.88	45.84	45.04	81.58	41.04	40.55
Occipital	45.14	22.44	22.70	48.38	24.15	24.23	42.30	20.94	21.36
Subcortical GM	38.83	19.38	19.46	40.33	20.15	20.18	37.52	18.70	18.82
Thalamus	14.45	7.20	7.25	14.91	7.43	7.47	14.04	6.99	7.05
Caudate nucleus	11.23	5.58	5.64	11.60	5.78	5.83	10.89	5.41	5.48
Putamen	10.67	5.38	5.29	11.25	5.69	5.56	10.16	5.11	5.05
Globus pallidus	2.49	1.21	1.28	2.57	1.25	1.32	2.42	1.18	1.24
Lateral ventricles	11.69	5.67	6.01	12.40	6.00	6.40	11.06	5.38	5.68
Cerebellum	132.82	66.12	66.71	138.85	69.10	69.75	127.53	63.50	64.03
Brainstem	29.32	—	—	30.69	—	—	28.11	—	—
B. CV (%)[b]									
Total brain volume[a]	9.08	—	—	7.92	—	—	8.51	—	—
Whole-brain GM	10.30	—	—	8.79	—	—	9.79	—	—
Whole-brain WM	13.86	—	—	12.99	—	—	12.35	—	—
Lobar GM	11.31	11.30	11.35	9.94	9.90	10.01	10.81	10.85	10.79
Frontal	11.20	11.23	11.25	9.68	9.66	9.79	10.84	10.93	10.83
Parietal	13.40	13.41	13.74	12.09	12.30	12.28	13.09	13.06	13.46
Temporal	10.97	11.22	10.96	9.94	10.30	9.85	10.33	10.54	10.39
Occipital	17.35	18.22	17.69	16.70	17.56	16.96	16.27	17.13	16.84
Lobar WM	14.62	14.62	14.67	13.48	13.44	13.58	13.36	13.34	13.42
Frontal	14.31	14.33	14.38	13.02	13.01	13.16	13.14	13.19	13.18
Parietal	15.48	15.57	15.74	14.03	14.38	14.01	14.79	14.68	15.31
Temporal	15.98	16.34	16.02	15.15	15.40	15.35	14.91	15.34	14.89
Occipital	18.77	19.48	19.07	18.32	18.56	19.08	16.55	17.55	16.64
Subcortical GM	8.24	8.29	8.33	7.64	7.60	7.81	7.18	7.20	7.32
Thalamus	9.10	9.09	9.39	9.04	8.95	9.48	8.15	8.17	8.38
Caudate nucleus	9.76	9.92	9.89	8.62	8.69	8.86	9.83	10.00	9.96
Putamen	11.67	11.88	11.90	11.05	10.97	11.49	9.87	10.17	10.18
Globus pallidus	13.26	15.46	13.45	13.46	16.37	13.01	12.41	14.06	13.15
Lateral ventricles	43.38	46.97	45.35	40.89	45.01	44.17	45.22	48.39	45.79
Cerebellum	10.06	10.04	10.22	9.29	9.25	9.47	8.95	8.97	9.08
Brainstem	10.93	—	—	10.45	—	—	9.56	—	—

T = RH + LH; RH = right hemisphere; LH = left hemisphere
[a]Total brain volume is defined as the sum of whole-brain GM and WM volumes.
[b]CV (%) = SD/mean × 100.

included parental education, AFI, and BMI. Preliminary analyses indicated that AFI and parent education had no significant relations with any regional brain volume (P values ranged from 0.27 to 0.98). These were therefore dropped from the final models. Recruitment and scan site (PSC) was also entered in the models to evaluate potential variation associated with scanning devices, but this variable was also found to be statistically insignificant and was dropped from the final models. Although fallback scans were more prevalent in younger children, this interaction, when added to the multivariable model, did not change the coefficients in Table 5 significantly and was dropped.

The models were constructed such that female volumes were designated as the baseline reference volume with subsequent coefficients indicating the percent increase or decrease relative to that baseline. For structures for which separate hemispheric volumes were available, female right hemisphere volume was designated as an arbitrary baseline reference, relative to which the coefficients indicate percent increase or decrease. Thus, for example, for parietal GM, the Hemisphere estimate (0.73) indicates that the left hemisphere volume was increased relative to the right by 0.73%. In addition, there is also a significant Sex by TBV interaction and a significant Sex by Hemisphere interaction, indicating that the male left parietal GM is larger still by another estimated 1.06%, less 0.02% after adjusting for TBV. Thus, the effects of multiple factors are considered simultaneously.

Higher-order terms were also tested in the models to evaluate potential nonlinear relationships between age and specific volumes. Thus, where a quadratic age term (Age^2) appears in Table 5, the relationship to age is not a simple linear function, but a curvilinear one (inverted-U shaped), similar to the shapes seen in Figure 1. Interactions between sex and the quadratic term were tested, but were not found to be statistically significant, even though different trajectories were fitted for the 2 sexes for all structures. The model selection criterion (the AIC) found that these interactions were less important than those included in the table based on best-fitting simplest models that included and excluded these coefficients. Higher-order polynomial terms were also tested, but none were found to be statistically significant.

Table 5 can be used to estimate normative volumes for specific regional structures when age, sex, TBV, and BMI are known. In the example shown below, we estimate the left temporal lobe GM volume of a healthy male 18.0 years of age with TBV of 1400 cm^3 and a BMI of 22.2. Note that no term is included for sex because it was not a significant predictor of temporal lobe GM following adjustment for TBV.

Male left temporal lobe GM volume =
(female right temporal lobe reference volume)
+ [(subject TBV − mean TBV) × (TBV percent change)]
+ [(subject left hemisphere indicator)
× (female right temporal reference volume)
× (hemisphere percent change)]
+ [(subject age − mean age) × (age percent change)]
+ [(subject BMI − mean BMI) × (BMI percent change)].

Upon substituting the appropriate values from Table 5,

Subject left temporal lobe GM volume
(male, aged 18.0, TBV 1400, BMI 22.2)
= 87.95
+ [(1400.00 − 1262.43) × 0.0007] + [(1) × (87.95)
× (−0.0225)] + [(18.0 − 10.9) × (−0.0070)] + [(22.2 − 19.2)
× (−0.0039)] = 89.96 cm^3.

The findings displayed in Table 5 are summarized below. Only findings that are statistically significant are addressed. Probability levels for statistical significance are indicated in the table by asterisks.

Total Brain Volume

As shown in Table 5, the mean TBV for males exceeded that of females by 10.28% overall. TBV increased by 2.03% per year in cross-sectional age ($P < 0.05$), offset by the significant decrease in TBV by quadratic age of –0.09% ($P < 0.05$), reflecting a curvilinear, age-related increase and then decrease (inverted U) in TBV across the age range. Whole-brain GM volume declined at approximately 6.56 cm^3 per year of age, whereas whole-brain WM increased by 6.49 cm^3 per year of age throughout the age range.

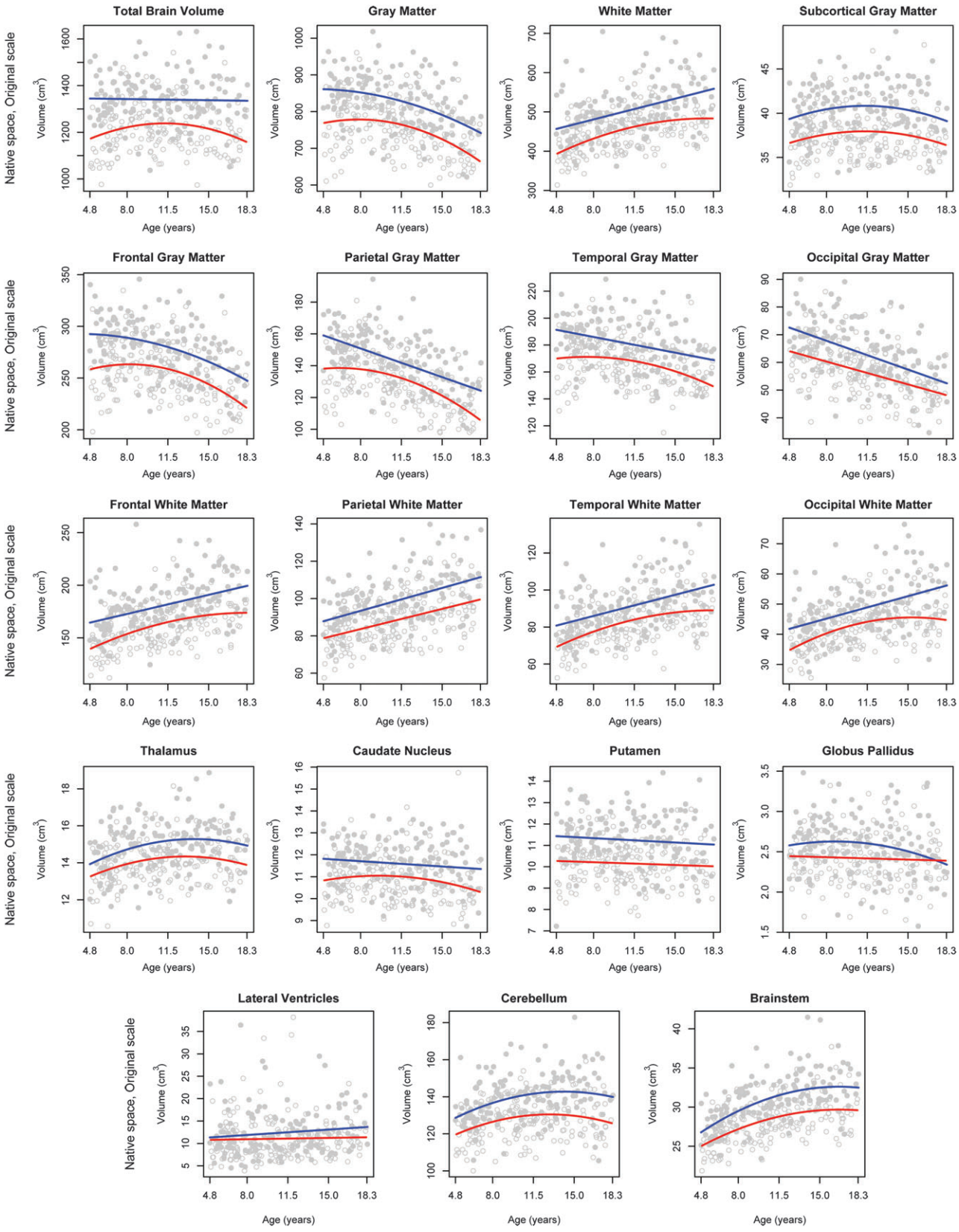

Figure 1. Individual data points and best-fitting cross-sectional age curves for males and females separately for all regional volumes without consideration of any other covariates.

Table 4

Means of regional brain structure volumes by age and sex expressed as a percent of 17- to 18-year-old volumes (cm^3)

Age in years (#male/#female)		4 (2/2)	5 (11/11)	6 (20/21)	7 (10/14)	8 (14/12)	9 (9/15)	10 (12/19)	11 (9/16)	12 (14/10)	13 (13/11)	14 (11/11)	15 (11/10)	16 (3/8)	17–18 (14/29)
Total brain[a]	Male	105.8	103.3	100.9	101.4	104.6	103.3	101.8	101.7	103.3	102.9	102.7	105.6	99.4	1308.22
	Female	83.7	89.5	96.5	99.1	98.3	98.2	94.6	99.6	96.8	96.9	93.0	93.3	92.8	1267.67
Whole-brain GM	Male	116.6	116.0	113.1	112.4	114.6	115.6	109.4	109.9	110.9	107.0	106.2	106.7	99.5	749.10
	Female	101.9	105.6	113.0	115.7	114.7	113.2	107.7	110.0	109.0	106.6	102.0	99.2	98.2	696.55
Whole-brain WM	Male	90.8	86.6	85.0	87.0	91.4	86.4	92.1	90.9	93.4	98.2	98.0	104.8	99.4	543.41
	Female	70.6	80.0	87.0	90.1	89.8	90.8	90.0	99.3	93.9	97.4	93.9	98.8	98.7	487.70
Subcortical GM	Male	100.5	101.8	102.6	107.4	104.6	104.6	104.0	105.1	103.5	105.5	104.4	106.7	100.8	38.77
	Female	91.8	96.8	102.8	102.9	102.4	103.3	101.0	102.6	101.4	101.2	99.4	102.4	99.7	37.01
Lateral ventricles	Male	119.2	82.4	77.4	80.4	87.1	110.5	76.1	92.2	89.5	75.4	106.1	85.6	96.9	14.01
	Female	55.5	81.0	103.9	92.1	81.3	111.3	85.6	109.7	88.5	92.5	94.2	82.4	97.2	11.70
Cerebellum	Male	94.3	95.5	94.6	97.8	99.1	103.9	99.3	99.4	101.3	104.0	102.9	107.1	100.0	138.95
	Female	85.6	93.4	95.7	100.6	102.8	101.3	99.9	99.7	100.2	102.1	98.9	98.8	99.1	128.37
Brainstem	Male	85.5	84.6	85.0	91.8	93.3	95.3	93.7	95.1	96.7	101.8	99.0	102.7	99.4	65.01
	Female	79.1	85.7	91.2	93.7	93.9	94.4	94.1	100.0	98.3	100.0	101.5	100.3	98.9	58.60

[a]Total brain volume is defined as the sum of whole brain GM and whole-brain WM.

Table 5

Results of mixed-effects regression models, showing covariates that are statistically significant predictors of regional brain volumes

Brain volume	Reference volume	Percent change and percent change per cross-sectional year from reference volume							
	Female right hemisphere	TBV[a] (mean: 1262.43 cm^3)	Hemisphere (left minus right)	Age (mean: 10.9 years)	Sex (male minus female)	Age^2	Body mass index (mean: 19.2)	Sex by TBV (male)	Sex by Hemisphere (left and male)
Total brain[a]	1204.86[b]			2.03*	10.28***	−0.09*			
Whole-Brain GM	787.13	0.08***		−0.87***			−0.19**		
Whole-Brain WM	475.30	0.09***		1.44***			0.33**	0.02*	
Lobar GM	318.96	0.08***		−1.11***			−0.19**		
Frontal	134.34	0.08***	−0.32**	−0.97***					
Parietal	68.43	0.09***	0.73*	−1.57***			−0.25*	−0.02*	1.06*
Temporal	87.95	0.07***	−2.25***	−0.70***			−0.39*		
Occipital	28.73	0.06***	5.26***	−1.92***	3.19*		−0.51*		
Lobar WM	196.93	0.09***	0.22*				0.32**		
Frontal	84.16	0.09***	0.65***	1.37***			0.33**		
Parietal	46.02	0.09***	0.60*			0.07*	0.26**		
Temporal	43.53	0.09***	−1.46**	1.64***			0.13*		
Occipital	21.93	0.08***	1.17**	2.14***				0.04**	
Subcortical GM	19.25	0.05***	0.79***		1.37*				−0.78**
Thalamus	7.30	0.06***	0.68***	1.64**		−0.05*			
Caudate nucleus	5.63	0.06***	1.13***	−0.28**					
Putamen	5.22	0.04***	−1.24***		5.33***				−1.26*
Globus pallidus	1.20	0.03***	5.30***	−0.38*					
Lateral Ventricles	5.86	0.16***							
Cerebellum	66.10	0.05***	0.89***	2.12**	2.03*	−0.07*			
Brainstem	29.38	0.06***		1.46***					

[a]Total brain volume is defined as the sum of whole-brain GM and whole-brain WM.

[b]Reference volume includes left and right hemispheres.

*$P < 0.05$, ** $P < 0.01$, *** $P < 0.001$.

Regional Brain Volumes

TBV, hemisphere, age, BMI, and to a lesser extent sex were all associated with variation in regional brain volumes when considered simultaneously in the context of the multivariable model. All regional volumes were positively correlated with TBV. The largest such association emerged for the lateral ventricles (0.16%). Coefficients were larger for lobar GM (0.08%) and WM (0.09%) than for subcortical GM structures (0.05%).

Age

As expected, after adjusting for TBV, lobar GM declined across age, by an estimated 1.11% per year of age, whereas lobar WM increased by an approximate 1.54% per year of age. There was more variability across relative regional lobar volumes for GM than WM. For GM, the age-related declines were far more prominent in the parietal and occipital cortex than in the frontal and temporal cortex. In contrast, for lobar WM, the rate of volumetric increase with age was relatively more consistent across structures, ranging from 1.37% (frontal) per year of age to 2.14% (occipital).

Age-related change was not detected, however, for the total subcortical GM or for the lateral ventricles. This summary measure of subcortical structures, however, masks an age-related increase for the thalamus and decreases for the caudate and globus pallidus. Although the age estimate for the ventricles was relatively large (0.98%), it failed to reach a level of statistical significance, presumably because of the high degree of interindividual variation, as indicated by the very large CV, shown in Table 4.

Sex

As noted previously, the most prominent finding with respect to sex was that TBV was approximately 10% larger in males than in females. The absence of a sex by age interaction suggests that this difference was relatively constant across the age range. All sex effects on regional volumes are reported after adjusting for TBV. Occipital GM volumes were larger by an estimated 3.2% in males relative to females. A sex difference in the putamen was especially striking, with the male volume larger by >5%. The cerebellum was approximately 2% greater in volume in males. There were also several small interactions of sex with TBV (Table 5).

Hemispheric Asymmetry

Significant hemispheric asymmetries were seen in both lobar and subcortical volumes. The frontal and temporal lobes showed a rightward GM asymmetry, whereas the parietal and occipital lobes showed a leftward GM asymmetry. The leftward asymmetry of occipital GM was especially pronounced, by approximately 5%. For lobar WM, there was a rightward asymmetry in the temporal lobe, in contrast to the leftward asymmetry seen for other lobar volumes.

Asymmetries were also seen in subcortical GM structures, most of which showed leftward asymmetry, the exception being the putamen, which was larger on the right. The asymmetry was most pronounced for the globus pallidus, by approximately 5%. Finally, the left lateral ventricle was larger than the right, by nearly 6%.

There were a few interactions between sex and hemisphere, but no significant interactions were found between age and hemisphere, suggesting that these asymmetries are relatively stable across the age range. A leftward parietal GM asymmetry was seen in both males and females but was more pronounced in males, as indicated by the significant sex × hemisphere interaction. The putamen showed a significant rightward asymmetry, which was more pronounced in males.

Body Mass Index

There were small but statistically significant and consistent associations of BMI with tissue-specific lobar brain volumes. A higher BMI was associated with smaller GM volumes and larger WM volumes, across age and sex, without any net impact on TBV. The largest such association was for occipital GM (–0.51%), but the association for occipital WM failed to reach statistical significance. BMI was not associated with variations in any other volumes.

Discussion

This study is, to our knowledge, the first pediatric MRI study to implement a population-based sampling strategy to generate unbiased estimates of global and regional brain volumes in a large sample of healthy children and adolescents, ages 4–18 years. It is also the first to examine comprehensively the effects of key socioeconomic indicators on healthy brain volumetric development and the first to report the effects of BMI on brain volumes in healthy children. We describe and quantify associations with age and sex for global brain volumes, regional brain volumes, and hemispheric asymmetries, as measured by multispectral MRI in conjunction with an automated processing pipeline, strict quality control, and a well-established biostatistical model.

There were minimal cross-sectional age-related differences in TBV within the 4- to 18-year-old age range, larger TBVs in males, age-related decreases in cerebral GM, concomitant increases in WM, and more prominent age-related differences in cortical structures and the cerebellum relative to subcortical structures. Salient leftward asymmetries (>1% of TBV) were seen in occipital GM, occipital WM, temporal WM, caudate, and globus pallidus, whereas a prominent rightward asymmetry was seen in temporal lobe GM. Neither of the 2 socioeconomic indicators examined here, AFI or parental education, was significantly related to the volumetric brain measures examined in this healthy pediatric sample. BMI index was inversely related to cerebral GM volumes and positively related to cerebral WM volumes, with no net effect on overall brain volume. We now discuss these findings in more detail.

TBV showed a very small, curvilinear pattern of association across the age range, first increasing and then decreasing very slightly, consistent with some previous reports (e.g., Giedd et al. 1996; Sporn et al. 2003; Lenroot et al. 2007). Thus, most of the increase in global brain volume has already occurred by approximately age 5, or early school age. TBV was approximately 10% greater in males than in females across the age range, also consistent with both the pediatric (Caviness et al. 1996; Giedd et al. 1996, 1999; Reiss et al. 1996; Lange et al. 1997; Kennedy et al. 1998) and adult (Cosgrove et al. 2007) literature. There is evidence that males, at birth, have approximately 9% larger intracranial volumes (including 10% more cortical GM and 6% more cortical WM) than do females (Gilmore et al. 2007), thus extending this sexual dimorphism to younger age ranges.

All regional volumes were significantly correlated with TBV, necessitating adjustment for overall brain size when making regional, and particularly male–female, comparisons. After such adjustment, considerable variability among regional volumes remained. Associations with TBV were generally larger for lobar GM and WM than for subcortical GM structures. Thus, linear stereotaxic normalization may obscure true, though subtle, relationships between regional, particularly cortical, measures and brain size, particularly during development.

Following adjustments for TBV, there were few sex differences, consistent with some, but not all (Sowell et al. 2002), earlier reports in children (Caviness et al. 1996; Giedd et al. 1996; Lange et al. 1997; Kennedy et al. 1998) and with data in adults (Luders et al. 2002). Thus, many reported sex differences may actually reflect differences in brain size. Only the relative volumes of occipital GM, putamen, and cerebellum differed significantly by sex, all larger in males. Some of these effects are consistent with prior reports (e.g., Giedd et al. 1996 reported larger putamen in males), but other previously reported sex differences were not detected. Among these nonreplicated findings are reports of proportionally larger GM volumes in females involving the frontal lobe (Lenroot et al. 2007) and the caudate (Giedd et al. 1996; Wilke et al. 2007). Inconsistencies likely arise from the high interindividual and interstudy variability seen across similar efforts, differences in the specific regional measures examined, sampling design, biostatistical models applied, and other methodological issues. The determinants and implications of any sex-related differences in brain volumes are unclear. Few studies have examined hormonal, genetic, or experiential influences on global brain size. Neither have the functional correlates of such differences been elucidated, and indeed our cognitive data revealed few sex differences (Waber et al. 2007).

Controlling for brain size may be critical when assessing variations in regional brain volumes and other cerebral measures, particularly when examining sex differences and/or disorders associated with deviations in brain size, such as autism spectrum disorders, which are associated with early brain overgrowth (Lainhart et al. 1997; Schumann et al. 2010), and ADHD, which is associated with smaller brain volumes (Valera et al. 2007). Few studies have controlled specifically and stringently for whole-brain volumes when examining regional structural variations. Sowell et al. (2007) is a notable exception, which matched a subset of subjects for brain size to confirm that sex differences identified in cortical thickness were independent of brain volume. Further allometric study of brain development in both health and neurodevelopmental disorders is warranted.

In contrast to the relative stability of TBVs, cortical GM and cerebral WM volumes showed dynamic relations with age. Global and regional GM volumes decreased and WM increased across the age range for nearly all regions reported here, in keeping with prior findings (Caviness et al. 1996; Reiss et al. 1996; Lange et al. 1997; Giedd et al. 1999). Only the putamen and lateral ventricles failed to show a significant relationship to age. The absence of a relation of age with the lateral ventricular volumes is most likely attributable to high between-subject variability, noted elsewhere in an independent sample (Lange et al. 1997).

When both sexes are analyzed together, most age-related associations (consisting of decreases in GM and increases in WM in most regions) were best described by linear functions, with curvilinear functions observed for TBV, parietal WM, thalamus, and cerebellum only. In the context of the more complex multiple regression model employed here, nonlinear relationships were less prominent than in earlier reports (Giedd et al. 1996; 1999). Within our sample, the numbers of subjects available were more sparse at the youngest and oldest ages, potentially limiting our ability to detect nonlinear relationships, as the identification of more complex functions requires more data points and parameters than those needed to fit simple linear functions (Van Belle and Fisher 2004). The observed trajectories did vary to some extent by sex; females tended to show curvilinear functions more often than did males. These sex differences merit further investigation using forthcoming longitudinal data from this sample. If confirmed, these sex differences should be explored in relationship to genetic, pubertal, and hormonal variables.

After adjusting for TBV, lobar GM declined across cross-sectional age by an estimated 1.11% per year of age, whereas lobar WM increased linearly by 1.54% per year. Age-related associations with GM were more variable across regions than those for WM. Declines in GM volumes were more prominent in parietal and occipital cortex than in frontal and temporal cortex, in keeping with a posterior-to-anterior sequence of maturation. In contrast, lobar WM showed a relatively consistent increase across lobar regions, except for the parietal lobe, ranging from 1.37% (frontal) to 2.14% (occipital) increase per year. These associations are generally consistent with previous reports (Giedd et al. 1996, 1999; Reiss et al. 1996; Sowell et al. 2002; Wilke et al. 2007).

The increases in WM and concurrent decreases in GM are consistent with progressive myelination and thinning of the cortical mantle reported from postmortem studies (Huttenlocher and Dabholkar 1997). The concomitant decreases in GM may reflect synaptic pruning. Although subcortical GM taken as a whole was not significantly associated with age, a substantial age-related increase was seen for the thalamus, along with smaller but statistically significant decreases for the caudate and globus pallidus. Overall, the relationship of age to volumes of the subcortical GM structures was more attenuated relative to the lobar volumes, reflecting a more protracted developmental course of cortical regions, despite the involvement of the basal ganglia in higher-order cognitive functions (Middleton and Strick 2000). In contrast with a previous report (Giedd et al. 1996), the cerebellum showed large volumetric increases through approximately age 11 years. Whether these various age-related differences in volumes also reflect varying capacities for experience-driven plasticity is unknown.

Hemispheric asymmetries were present in nearly every regional volume. Most reflected a larger volume on the left. Particularly salient were the leftward asymmetries of the occipital lobe, especially its GM, and temporal lobe WM, consistent with torque (the opposing tendency of the left posterior/right anterior brain to protrude further than its contralateral counterpart; LeMay 1976; Lancaster et al. 2003). Additional prominent leftward asymmetries were seen in the caudate and globus pallidus. Some leftward hemispheric asymmetries reported here contrast with an earlier report (Giedd et al. 1996) of rightward hemispheric asymmetries for the 4- to 18-year-old age range. Few studies have related global asymmetries to more local asymmetries or investigated their functional significance. However, a recent study reported a positive relationship of torque to asymmetries of the planum temporale (Barrick et al. 2005), shown to be related to handedness and language lateralization (Preis et al. 1999).

In contrast to these leftward asymmetries, temporal lobe GM showed a prominent rightward asymmetry, consistent with findings in adults (Jack et al. 1989) and the tendency of the Sylvian fissure to course upward posteriorly at a steeper angle on the right than on the left, although this asymmetry may be less pronounced in children than in adults (Sowell et al. 2001). Although such studies have primarily involved adults, alterations in cerebral asymmetries have been reported in neurodevelopmental disorders such as dyslexia (Zadina et al. 2006), schizophrenia (Sharma et al. 1999), and autism (Lange et al. 2010a) and thus may hold clinical significance.

There were no significant interactions between asymmetry and age, suggesting that these volumetric asymmetries are relatively stable across the age range. The only interactions of these asymmetries with sex involved parietal GM, which showed a more pronounced leftward asymmetry in males than in females, and the putamen, which showed a more pronounced rightward asymmetry. Although speculative, the enhanced parietal asymmetry in males may be related to sex differences in certain visuospatial skills (Wolbers and Hegarty 2010).

Socioeconomic indicators (family income and parental education) were not associated with variations in brain volumes in our analysis, consistent with a prior analysis indicating that total and regional brain volumes do not mediate the association between parental education and IQ in this sample (Lange et al. 2010b). Although there are scattered reports in which associations between socioeconomic variables and structural brain development have been examined, these have generally been in the context of studies designed to address specific circumscribed brain structures in small

samples of limited age range (Eckert et al. 2001; Raizada et al. 2008). To our knowledge, the present study is the first to conduct a comprehensive examination of regional and whole-brain volumes in relation to socioeconomic indicators in a large normative pediatric sample.

Socioeconomic status is a complex construct that has been associated with variation in life stress, social status, and neighborhood quality, as well as in child health and development (Evans and Kantrowitz 2002; Hackman and Farah 2009). Such associations likely reflect the combined and interactive influences of numerous environmental and biological influences, including genetic and epigenetic factors, whose effects may vary across the course of development.

Our stringent inclusion and exclusion criteria may also have contributed to the absence of association between socioeconomic indicators and volumetric MRI measures because the rate of health-based exclusions was significantly higher for lower-income participants in our study (Waber et al. 2007). This pattern is consistent with the higher rates of morbidity, including psychiatric morbidity, typically observed in lower-income populations (Kessler et al. 1994; Muntaner et al. 1998; Mackenbach et al. 2008). Indeed, a large proportion of low-income children who did not meet criteria for the study were excluded on the basis of elevated levels of behavioral symptoms, attention problems (as measured by the CBCL) being frequent. Certain family factors that were exclusionary criteria for our study, such as smoking and psychopathology in first-degree relatives, are also more prevalent in less well-educated individuals (Giovino 2002).

A novel finding was a relatively small but consistent association between BMI and tissue-specific lobar brain volumes, adjusted for all other covariates, including family income and parental education. Twelve percent of the sample was classified as obese by recent childhood norms, but none had diabetes or other diseases associated with obesity. An additional 14% were classified as overweight. Both of these percentages are lower than those observed by Singh et al. (2010) for US children in 2007, who reported a 16% obesity and 32% overweight rate for children from birth through 17 years in a large survey. Higher BMI was associated with decreased whole-brain and lobar GM and increased whole-brain and lobar WM volumes, with no net effect on TBV and no effect on subcortical GM structures, cerebellum, or brainstem. BMI findings here are similar to those reported in healthy adults, including elderly adults, which document negative associations between BMI and GM volumes in various cortical regions (Pannacciulli et al. 2006; Gunstad et al. 2008; Taki et al. 2008). Obesity has also been associated with increases in WM volume in some studies (Walther et al. 2010), an effect reported to be at least partially reversible with dieting (Haltia et al. 2007), suggesting that some such effects are malleable. The present findings, derived from a very well-documented population-based sample, indicating that associations between BMI and brain structure are present in childhood and adolescence, are provocative. The significance of these associations, in particular their functional significance, warrants further investigation.

Limitations

The relationships of brain volumes to age and sex described here are based on cross-sectional data and await refinement in future analyses of the complete, longitudinal data set. With respect to socioeconomic status, our recruitment relied on family income alone as a proxy and recruited from largely urban areas surrounding major medical centers, thereby excluding rural participants. Despite our rigorous geocoding recruitment strategy, the resulting parental educational levels were higher than expected, perhaps limiting extrapolation to less well-educated low-income populations.

Conclusions

Data from this normative longitudinal pediatric database provide a reference for studies of both healthy brain development and a wide range of brain disorders affecting children and adolescents. This report provides an analysis of volumetric data from the first cross-sectional time point for the NIH MRI Study of Normal Brain Development, which will serve as a reference for future users. Volumetric data from this time point replicate and further quantify several prior findings in healthy pediatric samples of decreasing GM, increasing WM, relatively stable TBVs, and greater age-related variance in lobar structures relative to subcortical structures across the 4- to 18-year-old age range. Male brains were approximately 10% larger than female brains across the age range and largely accounted for sex differences in regional brain volumes. Other specifics, however, such as the shape (linear vs. curvilinear) of several age-related functions, some sex and age relationships, and identified asymmetries differed from prior reports. Neither family income nor parental education was significantly associated with variations in the brain volumes examined here. However, BMI was inversely related to lobar (but not subcortical) GM volumes and positively associated with WM volumes. Further longitudinal and multimodal analyses will refine and expand on these findings and relate them to measures of cognitive and behavioral functioning.

Funding

This project was supported with Federal funds from the National Institute of Child Health and Human Development, the National Institute on Drug Abuse, the National Institute of Mental Health, and the National Institute of Neurological Disorders and Stroke (Contract #s N01-HD02-3343; N01-MH9-0002; N01-NS-9-2314, -2315, -2316, -2317, -2319, and -2320; and NS34783).

Data Access

Access to the NIH Pediatric MRI Data Repository is freely available to qualified researchers whose institutions are covered by a federalwise assurance, who are studying normal brain development, disorders or diseases, and/or developing image processing tools and who agree to the terms of the Data Use Certification. Please see www.NIH-PediatricMRI.org for specific information on how to apply for access.

Supplementary Material

Supplementary material can be found at: http://www.cercor.oxfordjournals.org/.

Notes

Special thanks to the NIH contracting officers for their support. We thank Janet E. Lainhart, MD, for her comments on an early manuscript.

We also acknowledge the important contribution and remarkable spirit of John Haselgrove, PhD (deceased).

Disclaimer: The views herein do not necessarily represent the official views of the National Institute of Child Health and Human Development, the National Institute on Drug Abuse, the National Institute of Mental Health, the National Institute of Neurological Disorders and Stroke, the NIH, the US Department of Health and Human Services, or any other agency of the US Government. *Conflict of Interest* : None declared.

Appendix: BDCG Authorship List

The MRI Study of Normal Brain Development is a cooperative study performed by DCC, a Clinical Coordinating Center, a Diffusion Tensor Processing Center, and staff of the National Institute of Child Health and Human Development (NICHD), the National Institute of Mental Health (NIMH), the National Institute on Drug Abuse (NIDA), and the National Institute for Neurological Diseases and Stroke (NINDS), Rockville, M.

Key personnel from the 6 pediatric study centers (PSCs) are as follows: **Children's Hospital Medical Center of Cincinnati**, Principal Investigator William S. Ball, MD, Investigators Anna Weber Byars, PhD, Mark Schapiro, MD, Wendy Bommer, RN, April Carr, BS, April German, BA, Scott Dunn, RT; **Children's Hospital Boston**, Principal Investigator Michael J. Rivkin, MD, Investigators Deborah Waber, PhD, Robert Mulkern, PhD, Sridhar Vajapeyam, PhD, Abigail Chiverton, BA, Peter Davis, BS, Julie Koo, BS, Jacki Marmor, MA, Christine Mrakotsky, PhD, MA, Richard Robertson, MD, Gloria McAnulty, PhD; University of Texas Health Science Center at Houston, Principal Investigators Michael E. Brandt, PhD, Jack M. Fletcher, PhD, Larry A. Kramer, MD, Investigators Grace Yang, MEd, Cara McCormack, BS, Kathleen M. Hebert, MA, Hilda Volero, MD; **Washington University in St. Louis**, Principal Investigators Kelly Botteron, MD, Robert C. McKinstry, MD, PhD, Investigators William Warren, Tomoyuki Nishino, MS, C. Robert Almli, PhD, Richard Todd, PhD, MD, John Constantino, MD; **University of California Los Angeles**, Principal Investigator James T. McCracken, MD, Investigators Jennifer Levitt, MD, Jeffrey Alger, PhD, Joseph O'Neill, PhD, Arthur Toga, PhD, Robert Asarnow, PhD, David Fadale, BA, Laura Heinichen, BA, Cedric Ireland BA; **Children's Hospital of Philadelphia**, Principal Investigators Dah-Jyuu Wang, PhD and Edward Moss, PhD, Investigators Robert A. Zimmerman, MD, and Research Staff Brooke Bintliff, BS, Ruth Bradford, Janice Newman, MBA. The Principal Investigator of the data coordinating center at **McGill University** is Alan C. Evans, PhD, Investigators Rozalia Arnaoutelis, BS, G. Bruce Pike, PhD, D. Louis Collins, PhD, Gabriel Leonard, PhD, Tomas Paus, MD, Alex Zijdenbos, PhD, and Research Staff Samir Das, BS, Vladimir Fonov, PhD, Luke Fu, BS, Jonathan Harlap, Ilana Leppert, BE, Denise Milovan, MA, Dario Vins, BC, and at **Georgetown University**, Thomas Zeffiro, MD, PhD, and John Van Meter, PhD. Corresponding author Nicholas Lange, ScD, **Harvard University/McLean Hospital**, is the biostatistical study design and data analysis Investigator to the DCC, assisted by Michael P. Froimowitz, MS. The Principal Investigator of the Clinical Coordinating Center at **Washington University** is Kelly Botteron, MD, Investigators C. Robert Almli, PhD, Cheryl Rainey, BS, Stan Henderson, MS, Tomoyuki Nishino, MS, William Warren, Jennifer L. Edwards, MSW, Diane Dubois, RN, Karla Smith, Tish Singer and Aaron A. Wilber, MS. The Principal Investigator of the Diffusion Tensor Processing Center at the National Institutes of Health (NIH) is Carlo Pierpaoli, MD, PhD, Investigators Peter J. Basser, PhD, Lin-Ching Chang, ScD, and Lindsay Walker, MS. The Principal Collaborators at the **NIH** are Lisa Freund, PhD (NICHD), Judith Rumsey, PhD (NIMH), Lauren Baskir, PhD (NIMH), Laurence Stanford, PhD (NIDA), Karen Sirocco, PhD (NIDA) and from NINDS, Katrina Gwinn-Hardy, MD, and Giovanna Spinella, MD. The Principal Investigator of the Spectroscopy Processing Center at the **University of California Los Angeles** is James T. McCracken, MD, Investigators Jeffry R. Alger, PhD, Jennifer Levitt, MD, Joseph O'Neill, PhD.

References

Akaike H. 1974. A new look at the statistical model identification. IEEE Trans Autom Contr. 19:716–723.

Almli CR, Rivkin MJ, McKinstry RC. Brain Development Cooperative Group. 2007. The NIH MRI study of normal brain development (Objective-2): newborns, infants, toddlers, and preschoolers. Neuroimage. 35:308–325.

Barrick TR, Mackay CE, Prima S, Maes F, Vandermeulen D, Crow TJ, Roberts N. 2005. Automatic analysis of cerebral asymmetry: an exploratory study of the relationship between brain torque and planum temporale asymmetry. Neuroimage. 24:678–691.

Brain Development Cooperative Group (corresponding author Evans AC). 2006. The NIH MRI study of normal brain development. Neuroimage. 30:184–202.

Caviness VS, Jr., Kennedy DN, Richelme C, Rademacher J, Filipek PA. 1996. The human brain age 7–11 years: a volumetric analysis based on magnetic resonance images. Cereb Cortex. 6:726–736.

Cocosco CA, Zijdenbos AP, Evans AC. 2003. A fully automatic and robust brain MRI tissue classification method. Med Image Anal. 7:513–527.

Collins DL, Evans AC. 1997. ANIMAL: validation and applications of nonlinear registration-based segmentation. Int J Pattern Recog Artif Intell. 11:1271.

Collins DL, Holmes CJ, Peters TM, Evans AC. 1995. Automatic 3D model-based neuroanatomical segmentation. Hum Brain Mapp. 3:190–208.

Collins DL, Neelin P, Peters TM, Evans AC. 1994. Automatic 3D intersubject registration of MR volumetric data in standardized Talairach space. J Comput Assist Tomogr. 18:192–205.

Cosgrove KP, Mazure CM, Staley JK. 2007. Evolving knowledge of sex differences in brain structure, function, and chemistry. Biol Psychiatry. 62:847–855.

Eckert MA, Lombardino LJ, Leonard CM. 2001. Planar asymmetry tips the phonological playground and environment raises the bar. Child Dev. 72:988–1002.

Evans GW, Kantrowitz E. 2002. Socioeconomic status and health: the potential role of environmental risk exposure. Annu Rev Public Health. 23:303–331.

Gedamu EL, Collins DL, Arnold DL. 2008. Automated quality control of brain MR images. J Magn Reson Imaging. 28:308–319.

Giedd JN, Blumenthal J, Jeffries NO, Castellanos FX, Liu H, Zijdenbos A, Paus T, Evans AC, Rapoport JL. 1999. Brain development during childhood and adolescence: a longitudinal MRI study. Nat Neurosci. 2:861–863.

Giedd JN, Snell JW, Lange N, Rajapakse JC, Casey BJ, Kozuch PL, Vaituzis AC, Vauss YC, Hamburger SD, Kaysen D, et al. 1996. Quantitative magnetic resonance imaging of human brain development: ages 4–18. Cereb Cortex. 6:551–560.

Gilmore JH, Lin W, Prastawa MW, Looney CB, Vetsa YS, Knickmeyer RC, Evans DD, Smith JK, Hamer RM, Lieberman JA, et al. 2007. Regional gray matter growth, sexual dimorphism, and cerebral asymmetry in the neonatal brain. J Neurosci. 27:1255–1260.

Giovino GA. 2002. Epidemiology of tobacco use in the United States. Oncogene. 21:7326–7340.

Gunstad J, Paul RH, Cohen RA, Tate DF, Spitznagel MB, Grieve S, Gordon E. 2008. Relationship between body mass index and brain volume in healthy adults. Int J Neurosci. 118:1582–1593.

Hackman DA, Farah MJ. 2009. Socioeconomic status and the developing brain. Trends Cogn Sci. 13:65–73.

Haltia LT, Viljanen A, Parkkola R, Kemppainen N, Rinne JO, Nuutila P, Kaasinen V. 2007. Brain white matter expansion in human obesity and the recovering effect of dieting. J Clin Endocrinol Metab. 92:3278–3284.

Harezlak J, Ryan LM, Giedd JN, Lange N. 2005. Individual and population penalized regression splines for accelerated longitudinal designs. Biometrics. 61:1037–1048.

Huttenlocher PR, Dabholkar AS. 1997. Regional differences in synaptogenesis in human cerebral cortex. J Comp Neurol. 387:167–178.

Jack CR, Jr., Twomey CK, Zinsmeister AR, Sharbrough FW, Petersen RC, Cascino GD. 1989. Anterior temporal lobes and hippocampal formations: normative volumetric measurements from MR images in young adults. Radiology. 172:549–554.

Kennedy DN, Lange N, Makris N, Bates J, Meyer J, Caviness VS Jr. 1998. Gyri of the human neocortex: an MRI-based analysis of volume and variance. Cereb Cortex. 8:372–384.

Kessler RC, McGonagle KA, Zhao S, Nelson CB, Hughes M, Eshleman S, Wittchen HU, Kendler KS. 1994. Lifetime and 12-month prevalence of DSM-III-R psychiatric disorders in the United States. Results from the National Comorbidity Survey. Arch Gen Psychiatry. 51:8–19.

Lainhart JE, Piven J, Wzorek M, Landa R, Santangelo S, Coon H, Folstein S. 1997. Macrocephaly in children and adults with autism. J Am Acad Child Adolesc Psychiatry. 36:282–290.

Laird NM, Ware JH. 1982. Random-effects models for longitudinal data. Biometrics. 38:963–974.

Lancaster JL, Kochunov PV, Thompson PM, Toga AW, Fox PT. 2003. Asymmetry of the brain surface from deformation field analysis. Hum Brain Mapp. 19:79–89.

Lange N, DuBray MB, Lee JE, Froimowitz MP, Froehlich A, Adluru N, Wright B, Ravichandran C, Fletcher PT, Bigler ED, et al. 2010a. Atypical diffusion tensor hemispheric asymmetry in autism. Autism Res. 3:350–358.

Lange N, Froimowitz MP, Bigler ED, Lainhart JE, Brain Development Cooperative Group. 2010b. Associations between IQ, total and regional brain volumes, and demography in a large normative sample of healthy children and adolescents. Dev Neuropsychol. 35:296–317.

Lange N, Giedd JN, Castellanos FX, Vaituzis AC, Rapoport JL. 1997. Variability of human brain structure size: ages 4–20 years. Psychiatry Res. 74:1–12.

Lange N, Laird NM. 1989. The effect of covariance structure on variance estimation in balanced growth curve models with random parameters. J Am Stat Assoc. 84:241–247.

LeMay M. 1976. Morphological cerebral asymmetries of modern man, fossil man, and nonhuman primate. Ann N Y Acad Sci. 280: 349–366.

Lenroot RK, Gogtay N, Greenstein DK, Wells EM, Wallace GL, Clasen LS, Blumenthal JD, Lerch J, Zijdenbos AP, Evans AC, et al. 2007. Sexual dimorphism of brain developmental trajectories during childhood and adolescence. Neuroimage. 36:1065–1073.

Luders E, Steinmetz H, Jancke L. 2002. Brain size and grey matter volume in the healthy human brain. Neuroreport. 13:2371–2374.

Mackenbach JP, Stirbu I, Roskam AJ, Schaap MM, Menvielle G, Leinsalu M, Kunst AE. 2008. Socioeconomic inequalities in health in 22 European countries. N Engl J Med. 358:2468–2481.

Middleton FA, Strick PL. 2000. Basal ganglia output and cognition: evidence from anatomical, behavioral, and clinical studies. Brain Cogn. 42:183–200.

Muntaner C, Eaton WW, Diala C, Kessler RC, Sorlie PD. 1998. Social class, assets, organizational control and the prevalence of common groups of psychiatric disorders. Soc Sci Med. 47:2043–2053.

Pannacciulli N, Del Parigi A, Chen K, Le DS, Reiman EM, Tataranni PA. 2006. Brain abnormalities in human obesity: a voxel-based morphometric study. Neuroimage. 31:1419–1425.

Preis S, Jancke L, Schmitz-Hillebrecht J, Steinmetz H. 1999. Child age and planum temporale asymmetry. Brain Cogn. 40:441–452.

Raizada RD, Richards TL, Meltzoff A, Kuhl PK. 2008. Socioeconomic status predicts hemispheric specialisation of the left inferior frontal gyrus in young children. Neuroimage. 40:1392–1401.

Reiss AL, Abrams MT, Singer HS, Ross JL, Denckla MB. 1996. Brain development, gender and IQ in children. A volumetric imaging study. Brain. 119(Pt 5):1763–1774.

Schumann CM, Bloss CS, Barnes CC, Wideman GM, Carper RA, Akshoomoff N, Pierce K, Hagler D, Schork N, Lord C, et al. 2010. Longitudinal magnetic resonance imaging study of cortical development through early childhood in autism. J Neurosci. 30:4419–4427.

Sharma T, Lancaster E, Sigmundsson T, Lewis S, Takei N, Gurling H, Barta P, Pearlson G, Murray R. 1999. Lack of normal pattern of cerebral asymmetry in familial schizophrenic patients and their relatives—the Maudsley Family Study. Schizophr Res. 40: 111–120.

Singh GK, Kogan MC, van Dyck C. 2010. Changes in state-specific childhood obesity and overweight prevalence in the United States from 2003 to 2007. Arch Pediatr Adolesc Med. 164:598–607.

Sled J, Zijdenbos A, Evans AC. 1998. A non-parametric method for automatic correction of intensity non-uniformity in MRI data. IEEE Trans Med Imaging. 17:87–97.

Smith SM. 2002. Fast robust automated brain extraction. Hum Brain Mapp. 17:143–155.

Sowell ER, Peterson BS, Kan E, Woods RP, Yoshii J, Bansal R, Xu D, Zhu H, Thompson PM, Toga AW. 2007. Sex differences in cortical thickness mapped in 176 healthy individuals between 7 and 87 years of age. Cereb Cortex. 17:1550–1560.

Sowell ER, Thompson PM, Mattson SN, Tessner KD, Jernigan TL, Riley EP, Toga AW. 2001. Voxel-based morphometric analyses of the brain in children and adolescents prenatally exposed to alcohol. Neuroreport. 12:515–523.

Sowell ER, Trauner DA, Gamst A, Jernigan TL. 2002. Development of cortical and subcortical brain structures in childhood and adolescence: a structural MRI study. Dev Med Child Neurol. 44:4–16.

Sporn AL, Greenstein DK, Gogtay N, Jeffries NO, Lenane M, Gochman P, Clasen LS, Blumenthal J, Giedd JN, Rapoport JL. 2003. Progressive brain volume loss during adolescence in childhood-onset schizophrenia. Am J Psychiatry. 160:2181–2189.

Taki Y, Kinomura S, Sato K, Inoue K, Goto R, Okada K, Uchida S, Kawashima R, Fukuda H. 2008. Relationship between body mass index and gray matter volume in 1,428 healthy individuals. Obesity. 16:119–124.

United States Census Bureau, 2000. SF1 and SF4, retrieved from: http://factfinder.census.gov.

United States Department of Housing and Urban Development's Office of Policy Development and Research, 2003. FY 2003 Income Limits..

Valera EM, Faraone SV, Murray KE, Seidman LJ. 2007. Meta-analysis of structural imaging findings in attention-deficit/hyperactivity disorder. Biol Psychiatry. 61:1361–1369.

Van Belle G, Fisher LD. 2004. Biostatistics: a methodology for the health sciences. Hoboken, NJ: Wiley-Interscience.

Venables VN, Ripley BD. 2002. Modern applied statistics with S. 4th ed. New York: Springer-Verlag.

Waber DP, De Moor C, Forbes PW, Almli CR, Botteron KN, Leonard G, Milovan D, Paus T, Rumsey J, Brain Development Cooperative Group. 2007. The NIH MRI study of normal brain development: performance of a population based sample of healthy children aged 6 to 18 years on a neuropsychological battery. J Int Neuropsychol Soc. 13:729–746.

Walther K, Birdsill AC, Glisky EL, Ryan L. 2010. Structural brain differences and cognitive functioning related to body mass index in older females. Hum Brain Mapp. 31:1052–1064.

Wilke M, Krageloh-Mann I, Holland SK. 2007. Global and local development of gray and white matter volume in normal children and adolescents. Exp Brain Res. 178:296–307.

Wolbers T, Hegarty M. 2010. What determines our navigational abilities? Trends Cogn Sci. 14:138–146.

Zadina JN, Corey DM, Casbergue RM, Lemen LC, Rouse JC, Knaus TA, Foundas AL. 2006. Lobar asymmetries in subtypes of dyslexic and control subjects. J Child Neurol. 21:922–931.

Zijdenbos AP, Forghani R, Evans AC. 2002. Automatic "pipeline" analysis of 3-D MRI data for clinical trials: application to multiple sclerosis. IEEE Trans Med Imaging. 21:1280–1291.